Effect of magnetic field on temporal development of Rayleigh -Taylor instability induced interfacial nonlinear structure

M. R. Gupta,* Labakanta Mandal,† Sourav Roy ‡, Manoranjan Khan§

Deptt. of Instrumentation Science & Centre for Plasma Studies

Jadavpur University, Kolkata-700032, India

Abstract

The effect of magnetic field on the nonlinear growth rate of Rayleigh - Taylor instability induced two fluid interfacial structures has been investigated. The magnetic field is assumed to be parallel to the plane of the two fluid interface and acts in a direction perpendicular to the wave vector. If magnetic field is restricted only to either side of the interface the growth rate may be depressed (may almost disappear) or be enhanced depending on whether the magnetic pressure on the interface opposes the instability driving pressure difference $g(\rho_h - \rho_l)$y or acts in the same direction. If magnetic field is present on both sides of the two fluid interface, stabilization

*e-mail: mrgupta_cps@yahoo.co.in

†e-mail: laba.kanta@yahoo.com

‡e-mail: phy.sou82@gmail.com

§e-mail: mkhan_ju@yahoo.com

may also take place in the sense that the surface of separation undulates periodically when the force due to magnetic pressure on two sides are such as to act in opposite direction. This result differs from the classical linear theory result which predicts that the magnetic field parallel to the surface has no influence on the growth rate when the wave vector is perpendicular to its direction.

I. INTRODUCTION

Temporal development of nonlinear structures at the two fluid interface consequent to Rayleigh - Taylor (RT) or Richtmyer - Meshkov (RM) instability is of much current interest both from theoretical and experimental point of view. The structure is called a bubble if the lighter fluid pushes across the unperturbed interface into the heavier fluid and a spike if the opposite takes place. The importance of such instabilities arises in connection with a wide range of problems ranging from astrophysical phenomena such as Supernova remnant to Inertial Confinement Fusion (ICF). A core collapse Super Nova (SN) is driven by an externally powerful shock, and strong shocks are the breeding ground of hydrodynamic instabilities like RT and RM instabilities. During the shock transit phase, the RM instability is activated at each discontinuity in the density profile of the star at the O-He and He-H interface. After shock transit, hydrodynamic mixing continues due to RT instability, as the denser layers are decelerated by lower density outer layer.

In an ICF situation, ablation front of an imploding capsule is subject to the RT instability because dense core is compressed and accelerated by low density ablating plasma. RT instability enhances the perturbation initiated by laser induced target non uniformity and consequently the performance of ICF implosion may be seriously affected. The dynamics of the instability of the interface of two constant density non-conducting fluids and the associated nonlinear structure has been studied by several authors [1]–[6] using an expression near the tip of the bubble or the spike up to second order in the transverse coordinate following Layzer's approach [7]. The fluids may also be ionized as in the astrophysical situation or may get ionized through laser irradiation in laboratory condition. Magnetic

field generated by ponderomotive force can exist [8]–[9] in such conducting (ionized) fluids and have important influence on the growth or suppression of the instabilities.

When the explosion of a Ia type supernova (SNIa) starts in a white dwarf as a laminar deflagration at the center of the star, RT instability begins to act [10],[11]. The burning velocity at these regimes can be described by fractal model of combustion. In white dwarf, magnetic field with strength upto $10^8 \sim 10^9$ G exist at the surface and the field near the center may be ~ 10 times greater. Rayleigh - Taylor instability arising during type Ia supernova explosion is associated with strong magnetic field. Since the magnetic field is dipolar type the fluid propagates parallel to the field lines (i.e., approximately along the direction of gravity) near the magnetic pole while the field lines are transverse to the direction of gravity at the magnetic equatorial region. Thus magnetic field effect on RT instability may have important roles to play whether the field lines are normal or parallel to the two fluid interface (i.e., along or perpendicular to the direction of gravity).

The effect of magnetic field on Rayleigh - Taylor instability has been studied in detail previously by Chandrasekhar [12]. When the magnetic field is normal to the surface of separation of the two fluids, the RT instability is almost unaffected by the magnetic field when the wave number 'k' of the perturbation is small; but contrary to the purely hydrodynamic case the growth rate does not increase indefinitely with 'k' but tends to a saturation value as $k \to \infty$. Magnetic field parallel to the direction of impulsively generated acceleration [13] is also shown to induce RM instability. This however happens for sufficiently intense magnetic field and also tends asymptotically to a saturation value.

In case the magnetic field is parallel to the surface of separation it is found that according to linear

theory there exists no effect of the magnetic field on the instability [12] if the latter is perpendicular to the wave vector $\vec{k}$. Non vanishing effect of transverse magnetic field with $\vec{k}$ perpendicular to the zeroeth order magnetic field is however found to exist in linear theory when compressibility effect is taken into account [14]. The growth rate is found to be lowered both for continuously accelerated (RTI) and impulsively accelerated (RMI) two fluid interface [15]–[22] when $\vec{k}$ has component parallel to the magnetic field. The nature of the depression has close resemblance to that due to surface tension [12] and also has useful application in astrophysical context [10],[23].

The present paper is addressed to the problem of the time development of the nonlinear interfacial structure caused by Rayleigh Taylor instability in presence of a magnetic field parallel to the surface of separation of the two fluids . The wave vector is assumed to lie in the same plane and perpendicular to the magnetic field. With such a geometry there is no effect of the magnetic field in the classical [12] linear approximation. However, it is no longer the case when linearization restriction is lifted. This may be understood from the following consideration.

In presence of magnetic field, there exists the magnetic pressure in addition to the usual hydrodynamic pressure. As a result the RT instability driving pressure difference $g(\rho_h - \rho_l)$y is changed by the inclusion of the magnetic pressure difference $(1/2\mu)(B_h^2 - B_l^2)$ [the suffix h(l) correspond to the dynamical variable associated with the heavier (lighter) fluid]. This has the consequence that the growth rate may be enhanced or depressed according as the extra contribution is either positive or negative . Moreover, as we shall see there may also occur stabilization in the sense that the surface of separation executes periodic undulation resulting from time lag in the temporal variation of B_h and B_l. It is interesting to note that these are entirely nonlinear effects and disappear in the linear

approximation.

Section II deals with the basic MHD equation together with the geometry involved. The fluid is assumed inviscid and perfectly conducting and the fluid motion to be one of potential type motion. The investigation of the nonlinear aspect of the mushroom structure of the two fluid interface is facilitated by Bernoulli's equation - the first integral of the equation of motion of the magnetofluid obtained with the help of the magnetic field geometry. The kinematical and dynamical boundary conditions holding at the two fluid interface are set forth in section III. The set of equations describing the temporal development of the RT instability induced nonlinear structures at the interface are derived in section IV. As these equation are not amenable to solution in closed analytic form, the results are obtained by numerical methods followed by graphical results and are presented in section V. A summary of the results is given in section VI.

II. BASIC EQUATIONS

Assume that the undisturbed surface is $y = 0$, the transverse coordinates being represented by x, z. The heavier fluid (density ρ_h =constant) occupies the region $y > 0$ while the lighter fluid (density ρ_l =constant) is in the region $y < 0$; gravity is taken to point along negative y axis.

As shown in Fig. 1, the magnetic field is taken along the z direction:

$$\vec{B} = \hat{z}B_h(x, y, t); \qquad y > 0 \tag{1}$$

$$= \hat{z}B_l(x, y, t); \qquad y < 0$$

so that $\vec{\nabla}.\vec{B} = 0$ (2)

automatically. The mushroom shaped perturbation interface which is called a bubble or a spike according as the lighter fluid pushes into the heavier fluid or the opposite is taken to have a parabolic form :

$$y(x,t) = \eta_0(t) + \eta_2(t)x^2 \tag{3}$$

Thus we have

$$\text{for a bubble:} \qquad \eta_0 > 0 \quad \text{and} \quad \eta_2 < 0 \tag{4}$$

$$\text{for a spike:} \qquad \eta_0 < 0 \quad \text{and} \quad \eta_2 > 0 \tag{5}$$

For uniform density fluid the equation of continuity $\vec{\nabla}.\vec{v} = 0$ is satisfied for irrotational fluid motion. Following Goncharov [5] the velocity potentials describing the irrotational motion for the heavier and lighter fluids are assumed to be given by

$$\phi_h(x,y,t) = a_1(t)\cos(kx)e^{-k(y-\eta_0(t))}; \quad y > 0 \tag{6}$$

$$\phi_l(x,y,t) = b_0(t)y + b_1(t)\cos(kx)e^{k(y-\eta_0(t))}; \quad y < 0 \tag{7}$$

$$\text{with } \vec{v}_{h(l)} = -\vec{\nabla}\phi_{h(l)}. \tag{8}$$

The fluid motion is governed by the ideal magneto hydrodynamic equations

$$\rho_{h(l)}\left[\frac{\partial \vec{v}_{h(l)}}{\partial t} + (\vec{v}_{h(l)}.\vec{\nabla})\vec{v}_{h(l)}\right] = -\vec{\nabla}p_{h(l)} - \rho_{h(l)}\vec{g} + \frac{1}{\mu_{h(l)}}(\vec{\nabla} \times \vec{B}_{h(l)}) \times \vec{B}_{h(l)} \tag{9}$$

$$\frac{\partial\vec{B}_{h(l)}}{\partial t}=\vec{\nabla}\times[\vec{v}_{h(l)}\times\vec{B}_{h(l)}] \tag{10}$$

For magnetic field of the form given by Eq. (1)

$$\frac{1}{\mu_{h(l)}}(\vec{\nabla}\times\vec{B}_{h(l)})\times\vec{B}_{h(l)}=\frac{1}{\mu_{h(l)}}(\vec{B}_{h(l)}.\vec{\nabla})\vec{B}_{h(l)}-\frac{1}{2\mu_{h(l)}}\vec{\nabla}(\vec{B^2}_{h(l)}) \tag{11}$$

Substitution for $\vec{v}_{h(l)}$ from Eq. (8) in Eq. (9) followed by use of Eq. (11) leads to Bernoulli's equation for the MHD fluid

$$-\frac{\partial\phi_{h(l)}}{\partial t}+\frac{1}{2}(\vec{\nabla}\phi_{h(l)})^2=-\frac{p_{h(l)}}{\rho_{h(l)}}-gy-\frac{1}{2\mu_{h(l)}\rho_{h(l)}}B^2_{h(l)}+\frac{f_{h(l)}(t)}{\rho_{h(l)}} \tag{12}$$

III. KINEMATICAL AND DYNAMICAL BOUNDARY CONDITIONS

The kinematical boundary conditions satisfied by the interfacial surface $y=\eta(x,t)$ are

$$\frac{\partial\eta}{\partial t}+(v_h)_x\frac{\partial\eta}{\partial x}=(v_h)_y \tag{13}$$

$$(v_h)_x\frac{\partial\eta}{\partial x}-(v_l)_x\frac{\partial\eta}{\partial x}=(v_h)_y-(v_l)_y \tag{14}$$

From Bernoulli's Eq. (12) for the heavier and lighter fluids one obtains the following equation

$$\begin{aligned}\rho_h[-\frac{\partial\phi_h}{\partial t}+\frac{1}{2}(\vec{\nabla}\phi_h)^2]-\rho_l[-\frac{\partial\phi_l}{\partial t}+\frac{1}{2}(\vec{\nabla}\phi_l)^2]=-[g(\rho_h-\rho_l)y+(p_h-p_l)\\+(\frac{B^2{}_h}{2\mu_h}-\frac{B^2{}_l}{2\mu_l})]+f_h(t)-f_l(t)\end{aligned} \tag{15}$$

Further with the help of Eqs. (1) and (2) and the incompressibility condition $\vec{\nabla}.\vec{v_{h(l)}} = 0$, Eq. (11) simplifies to

$$\frac{\partial[\vec{B}_{h(l)}(x,y,t)]}{\partial t} + (\vec{v}_{h(l)}.\vec{\nabla})\vec{B}_{h(l)} = 0 \tag{16}$$

The interfacial kinematic boundary conditions (13) and (14) together with Bernoulli's Eq. (15) and magnetic induction Eq. (16) are employed in the next section to obtain the temporal evolution of the elevation of the tip of bubble (spike) like structures at the two fluid interface from its undisturbed level.

IV. EQUATION FOR RAYLEIGH - TAYLOR INSTABILITY INDUCED INTERFACIAL STRUCTURE PARAMETERS

Substituting $\eta(x,t)$ and $\phi_{h(l)}(x,y,t)$ from Eqs.(3),(6)-(8) in Eqs. (13) and (14) and expanding in powers of the transverse coordinate x up to i=2 and neglecting terms O$(x^i)(i \geq 3)$, we obtain the following equations [22]

$$\frac{d\xi_1}{d\ t} = \xi_3 \tag{17}$$

$$\frac{d\xi_2}{d\ t} = -\frac{1}{2}(6\xi_2 + 1)\xi_3 \tag{18}$$

$$b_0 = -\frac{6\xi_2}{(3\xi_2 - \frac{1}{2})} k a_1 \tag{19}$$

$$b_1 = \frac{(3\xi_2 + \frac{1}{2})}{(3\xi_2 - \frac{1}{2})} a_1 \tag{20}$$

$$\xi_1 = k\eta_0; \qquad \xi_2 = \eta_2/k; \qquad \xi_3 = k^2 a_1 \tag{21}$$

ξ_1 and ξ_2 are respectively the nondimensionalized (with respect to the wave length) displacement and curvature of the tip of the bubble (spike) and ξ_3/k is tip velocity.

At this stage it is in order to justify neglect of contribution from terms of order $x^i (i \geq 3)$ as done here. This is provided on two counts:

(i) The interface displacement $y(x,t)$ is expanded in Eq. (3) keeping only terms of order x^2,-the customary practice in Layzer's approach. Since we are interested only in the motion close to the tip of the bubble or spike,i.e., for $x \approx 0$ it is sufficient to retain terms up to order x^2 and neglect $O(x^i)(i \geq 3)$.

(ii) Even if $\eta(x,t)$ is expanded as

$$\eta(x,t) = \eta_0(t) + \eta_2(t)x^2 + \eta_4(t)x^4 + \eta_6(t)x^6 ....$$

it can be shown that at the saturation level ($d\eta_i/dt = 0$) contributions from terms containing η_4, η_6...are much smaller than that from $\eta_2(t)$(see Appendix). Thus expansion of the kinematic condition and in its turn the expansion in Bernoulli's equation and Faraday's equation (which follows later) retaining higher order terms $O(x^4)$ can also be neglected.

Next let us turn to the magnetic field induction Eq. (16). To satisfy Eq. (16) with $\vec{v}_h$ given by Eq. (8) we set

$$B_h(x,y,t) = \beta_{h0}(t) + \beta_h(t)\cos(kx)e^{-k(y-\eta_0(t))}; \quad y > 0 \tag{22}$$

in Eq. (16); this leads to

$$\dot{\beta}_{h0}(t) + (\dot{\beta}_h(t) + \beta_h(t)k\dot{\eta}_0)\cos(kx)e^{-k(y-\eta_0(t))} - k^2 a_1 \beta_h e^{-2k(y-\eta_0(t))} = 0 \tag{23}$$

Corresponding to the parabolic interfacial structure represented by $y(x,t) = \eta_0(t) + \eta_2(t)x^2$ the foregoing equation yields on equating coefficients of x^i $(i = 0, 2)$ and neglecting terms $O(x^i)$with $i \geq 3$ the following relation

$i = 0: \quad \dot{\beta}_{h0}(t) + \dot{\beta}_h(t) = 0$

so that

$$\beta_{h0}(t) + \beta_h(t) = constant = B_{h0}, say \tag{24}$$

$i = 2:$

$$\frac{\delta \dot{B}_h}{\delta B_h(t)} = \frac{(\xi_2 - \frac{1}{2})}{(\xi_2 + \frac{1}{2})}\xi_3; \quad \delta B_h(t) = \frac{\beta_h(t)}{B_{h0}} \tag{25}$$

$$\delta B_h(t) = \delta B_h(t=0)\exp\left[\int_0^t \xi_3 \frac{(\xi_2 - \frac{1}{2})}{(\xi_2 + \frac{1}{2})}d\tau\right] \tag{26}$$

so that $\delta B_h(t=0) > (< 0)$; according as $\delta B_h(t=0) > (< 0)$.

In obtaining Eqs. (24) and (25) we have used the relation $\xi_3 = \dot{\xi}_1 = k\dot{\eta}_0 = k^2 a_1$ (Eq. (17)).

Similarly, to satisfy the magnetic field induction equation in the region $y < 0$, i.e., in the region occupied by the lighter fluid we set

$$B_l(x,y,t) = \beta_{l0}(t) + \beta_l(t)\cos(kx)e^{k(y-\eta_0(t))}; \tag{27}$$

and proceeding as in case of the magnetic field induction $B_h(x,y,t)$in region $y>0$, we obtain

$$\beta_{l0}(t)+\beta_l(t)=constant=B_{l0}, say \tag{28}$$

and

$$\frac{\delta\dot{B}_l}{\delta B_l(t)}=\frac{(\xi_2+\frac{1}{2})}{(\xi_2-\frac{1}{2})}\frac{(\xi_2+\frac{1}{6})}{(\xi_2-\frac{1}{6})}\xi_3; \quad \delta B_l(t)=\frac{\beta_l(t)}{B_{l0}} \tag{29}$$

by using Eqs. (19) and (20)($\Longrightarrow b_0+kb_1+ka_1=0$).

Again proceeding as in the deduction of Eq. (26) we obtain

$$\delta B_l(t)=\delta B_l(t=0)exp\left[\int_0^t \xi_3\frac{(\xi_2+\frac{1}{2})}{(\xi_2-\frac{1}{2})}\frac{(\xi_2+\frac{1}{6})}{(\xi_2-\frac{1}{6})}d\tau\right] \tag{30}$$

so that $\delta B_l(t=0)>(<0)$; according as $\delta B_l(t=0)>(<0)$.

The magnetic field affected Rayleigh - Taylor instability induced growth of the mushroom shaped surface structure are determined by the parameters $\xi_1(t),\xi_2(t),\xi_3(t)$ as also the magnetic induction perturbation $\delta B_h(t)$ and $\delta B_l(t)$. To determine the time evolution of these five functions we need aside from the differential Eqs. (17),(18),(25) and (29) an extra one to complete the set. This is provided by Eq. (15). Now using Eqs. (22) and (24) one obtains

$$\frac{1}{2\mu_h}B_h^2(x,y,t)=\frac{B_{h0}^2}{2\mu_h}-k^2\frac{B^2{}_{h0}}{\mu_h}\delta B_h(t)(\xi_2+\frac{1}{2})x^2 \tag{31}$$

Similarly using Eqs. (27) and (28) one obtains

$$\frac{1}{2\mu_l}B_l^2(x,y,t)=\frac{B_{l0}^2}{2\mu_l}+k^2\frac{B^2{}_{l0}}{\mu_l}\delta B_l(t)(\xi_2-\frac{1}{2})x^2 \tag{32}$$

where

$$\mid\delta B_h(t)\mid,\mid\delta B_l(t)\mid\ll 1 \tag{33}$$

whenever the initial values $\mid \delta B_h(0) \mid$ and $\mid \delta B_l(0) \mid \ll 1$ as may be seen from Eqs. (26) and (30). This anticipation is substantiated later by numerical computation (Fig. 2 -Fig. 5).

We next substitute for $B_h^2(x,y,t)/2\mu_h - B_l^2(x,y,t)/2\mu_l$ from Eqs. (31) and (32) in Eq. (16) and use the dynamical boundary condition expressing balance of fluid and finite order magnetic pressure on two sides of the interface:

$$p_h + \frac{B_{h0}^2}{2\mu_h} = p_l + \frac{B_{l0}^2}{2\mu_l} \tag{34}$$

Eq. (15) now reduces to

$$\begin{aligned}\rho_h[-\frac{\partial\phi_h}{\partial t} + \frac{1}{2}(\vec{\nabla}\phi_h)^2] - \rho_l[-\frac{\partial\phi_l}{\partial t} + \frac{1}{2}(\vec{\nabla}\phi_l)^2] = -g(\rho_h - \rho_l)y + k^2\frac{B_{h0}^2}{\mu_h}\delta B_h(t)(\xi_2 + \frac{1}{2})x^2 \\ + \frac{B_{l0}^2}{\mu_l}\delta B_l(t)(\xi_2 - \frac{1}{2})x^2 + f_h(t) - f_l(t)\end{aligned} \tag{35}$$

which involves the influence only of the infinitesimal magnetic field fluctuation on the interfacial structure. After some lengthy but straightforward algebraic manipulation we arrive at the required equation which is the last Eq. of the following set of Eqs. (36). The last Eq. of the set of Eqs. (36) is the required one as mentioned before and represents the dynamical boundary condition and obtained by setting $y = \eta_0 + \eta_2 x^2$ and equating coefficient of x^2 on both sides. All the equations are collected together below for the sake of convenience.

$$
\begin{aligned}
\frac{d\xi_1}{d\tau} &= \xi_3/\sqrt{kg} \\
\frac{d\xi_2}{d\tau} &= -\frac{1}{2}(6\xi_2+1)\xi_3/\sqrt{kg} \\
\frac{\frac{d}{d\tau}\delta B_h(t)}{\delta B_h(t)} &= \frac{(\xi_2-\frac{1}{2})}{(\xi_2+\frac{1}{2})}\xi_3/\sqrt{kg} \\
\frac{\frac{d}{d\tau}\delta B_l(t)}{\delta B_l(t)} &= \frac{(\xi_2+\frac{1}{2})}{(\xi_2-\frac{1}{2})}\frac{(\xi_2+\frac{1}{6})}{(\xi_2-\frac{1}{6})}\xi_3/\sqrt{kg} \\
\frac{d\xi_3}{d\tau} &= -\frac{N(\xi_2,r)}{D(\xi_2,r)}\frac{(\xi_3/\sqrt{kg})^2}{(6\xi_2-1)} + 2(r-1)\frac{\xi_2(6\xi_2-1)}{D(\xi_2,r)} \\
&\quad -\frac{(6\xi_2-1)}{D(\xi_2,r)}[r\frac{kV_h^2}{g}\delta B_h(t)(2\xi_2+1) + \frac{kV_l^2}{g}\delta B_l(t)(2\xi_2-1)]
\end{aligned}
\tag{36}
$$

$$
where, \tau = t\sqrt{kg}; \quad r = \frac{\rho_h}{\rho_l}; \quad D(\xi_2,r) = 12(1-r)\xi_2^2 + 4(1-r)\xi_2 + (r+1);
$$

$$
N(\xi_2,r) = 36(1-r)\xi_2^2 + 12(4+r)\xi_2 + (7-r) \tag{37}
$$

$$
V_{h(l)} = \sqrt{B^2_{h0(l0)}/\rho_{h(l)}\mu_{h(l)}} \tag{38}
$$

is the Alfven velocity in the heavier (lighter) fluid.

The above set of Eqs. describe the time evolution of a bubble. The time evolution of a spike is obtained from the same set by making the transformation $\xi_1 \to -\xi_1, \xi_2 \to -\xi_2$ and $r \to \frac{1}{r}$[5]. It is important to note that in the last Eq. of the set of Eqs.(36) the contribution to the bubble tip velocity $\frac{d\xi_3}{d\tau}$ from the force of buoyancy $g(\rho_h-\rho_l)$y is proportional to $kg(\rho_h-\rho_l)\xi_2$ while that from the magnetic pressure fluctuation are proportional to $k^2(B_{l0}^2/\mu_l)\delta B_l(t)(\xi_2-\frac{1}{2})$ and $k^2(B_{h0}^2/\mu_h)\delta B_h(t)(\xi_2+\frac{1}{2})$ respectively as may be seen from Eqs. (31) and(32). Further both for bubbles and spikes ξ_2 lies in $(-\frac{1}{6},\frac{1}{6})$; hence we always have $(\xi_2-\frac{1}{2})<0$ and $(\xi_2+\frac{1}{2})>0$. So by applying condition Eq. (30)

we find

$$k^2 \frac{B_{l0}^2}{\mu_l} \delta B_l(t)(\xi_2 - \frac{1}{2}) < or > 0; \tag{39}$$

according as $\delta B_l(t=0) > or < 0$.

Similarly on applying Eq. (26) it follows that

$$k^2 \frac{B_{h0}^2}{\mu_h} \delta B_h(t)(\xi_2 + \frac{1}{2}) > or < 0; \tag{40}$$

according as $\delta B_h(t=0) > or < 0$.

V. RESULTS AND DISCUSSIONS

Analytical closed form solution of the set of Eqs. (36) not being feasible we take recourse to the method of numerical solution (5th order Runge-Kutta-Fehlberg method) and consider the following cases.

Case A

Assume $B_{h0} = 0$, $B_{l0} \neq 0$. Such a situation may occur when the lighter fluid (occupying the lower region $y < 0$) is ionized while the heavier fluid (region $y > 0$) is nonmagnetic. From Eqs. (32) and (36) and the concluding discussions of the foregoing section it is clearly seen that the instability driving pressure difference $g(\rho_h - \rho_l)\xi_2$ is lowered or enhanced by $\mid k^2 \frac{B_{l0}^2}{\mu_l} \delta B_l(t)(\xi_2 - \frac{1}{2})\mid$ according as $\delta B_l(t=0)$ is > 0 or < 0. The concomitant growth rate modifications are shown in Fig. 2 (Fig. 3) which plots the bubble (spike) tip elevation $\mid \xi_1 \mid$ and growth rate $\mid \dot{\xi_1} \mid$. Fig. 2 and Fig. 3 show that whether in case of suppression or enhancement the growth rate $\xi_3(=\mid \dot{\xi_1} \mid)$ approaches an asymptotic

value as $\tau \to \infty$ both for bubble and for spike. This happens as $\delta B_l(t)$ exhibits similar asymptotic behavior as one may see in Fig. 2 and Fig. 3. The following analytic expressions for $(\xi_3)_{asymp}$ as $\tau \to \infty$ are obtained by setting $d\xi_3/d\tau = 0$ together with $B_{h0} = 0$ in the last Eq. of the set of Eqs. (36):

$$[(\xi_3)_{asymp}]_{bubble} = \sqrt{\frac{2Akg}{3(1+A)}}\sqrt{1 - 2(\frac{1-A}{A})\frac{kV_l^2}{g}[\delta B_l(\infty)]_{bubble}} \tag{41}$$

$$[(\xi_3)_{asymp}]_{spike} = \sqrt{\frac{2Akg}{3(1-A)}}\sqrt{1 - 2(\frac{1+A}{A})\frac{kV_l^2}{g}[\delta B_l(\infty)]_{spike}} \tag{42}$$

Here $\delta B_l(\infty)$denotes the asymptotic value. The growth rate increases (destabilization) if $\delta B_l(0) < 0$ (hence $\delta B_l(\infty) < 0$),i.e., the magnetic field perturbation diminishes the pressure below the interface relative to that above. On the other hand $(\xi_3)_{asym}$ decrease and asymptote to 0 (zero) as kV_l^2/g increases if $\delta B_l(0) > 0$ and therefore $\delta B_l(\infty) > 0$,i.e., the pressure below the interface increases and tends to restore stability.

Case B

Assume $B_{h0} \neq 0$ but $B_{l0} = 0$. This situation is the reverse of that in case **A** and may arise when the heavier fluid is ionized while the lighter one is non magnetic. The dynamical boundary condition shows that following the same line of arguments as in case **A** but with $B_{h0} \neq 0$ but $B_{l0} = 0$ we find that the instability driving force $g(\rho_h - \rho_l)\xi_2$ is now enhanced or reduced by $\mid k^2 \frac{B_{h0}^2}{\mu_h}\delta B_h(t)(\xi_2 + \frac{1}{2})\mid$ according as $\delta B_h(t=0)$ is $>$ or $<$ 0. This conclusion is supported by the difference in the height of the bubble (or spike) tip shown in Fig. 4 and Fig. 5. However note that $\delta B_h(t) \to 0$ as $t \to \infty$. This has the consequence that the asymptotic value of the velocity of the tip of the bubble (in spike)

height $(\xi_3)_{asymp}$ is the same as in the absence of magnetic field. But as $\mid \dot{\xi_1} \mid = \xi_3$ the height of the tip of the bubble (or spike) maintains a constant difference.

Case C Assume both fluids are conducting and magnetic field is non zero on either side. We have considered two cases

(i) $r\frac{k}{g}V_h^2 = \frac{k}{g}V_l^2 = 5.0$

(ii)$r\frac{k}{g}V_h^2 = 5.0, \frac{k}{g}V_l^2 = 10.0$

(iii)$r\frac{k}{g}V_h^2 = \frac{k}{g}V_l^2 = 1.2$

(iv)$r\frac{k}{g}V_h^2 = \frac{k}{g}V_l^2 = 1.4$

with $\delta B_h(t = 0) = \delta B_l(t = 0) > 0$ in each case. The bubble tip elevation ξ_1 as well as its velocity $\dot{\xi_1} = \xi_3$ oscillates as the magnetic pressure acts on both sides of the interfaces but in opposite direction and with opposite phase. The results are shown in Fig. 6. In (i) and also in (iii) and (iv) the growth rate $\xi_3 = \dot{\xi_1}$ oscillates approximately symmetrically about $\xi_3 = 0$ as $r\frac{k}{g}V_h^2 = \frac{k}{g}V_l^2$ equation for in $\dot{\xi_3}$ in set of Eqs. (36); in (ii) the asymmetry results from difference in the driving pressure difference on two sides. Moreover it is to be noted from Fig. 7 and Fig. 8 that the oscillation frequency increases with 'k' and also with Alfven velocity. Occurrence of such an oscillation were also concluded for RMI [19],[21] with increase in frequency similar to our case; however such oscillation are harmonic as against the nonlinear oscillations in our case.

VI. SUMMARY

Finally we summarize the results :

The change in interfacial pressure difference due to magnetic field fluctuation leads to enhancement or suppression of instability as stated below.

(i) If $B_{h0} = 0$,i.e, there exists no magnetic field above the two fluid interface ($y > 0$) but $B_{l0} \neq 0$ the lowering of the magnetic field below the interface $y = 0$ due to an initial perturbation $\delta B_l(0) < 0 (\Rightarrow \delta B_l(t) < 0$ (by Eq. (30)) according to the fourth Eq. of the set of Eqs. (36)) leads to depression of pressure on the side of the lighter fluid with the result that the instability growth is enhanced (Fig. 2). On the other hand if the initial perturbation $\delta B_l(0) > 0 (\Rightarrow \delta B_l(t) > 0$ (by Eq. (30)) the pressure on the side of the lighter fluid increases with resulting suppression of growth rate which asymptote to 0 (zero) as $(\frac{kV_l^2}{g})$ increases (Fig. 3).

$\delta B_l(t)$ tends to a constant value asymptotically as $t \to \infty$; this enables us to obtain an analytic expression for the asymptotic growth rate $(\xi_3)_{asym}$ both for bubble and spike as given by Eqs. (41) and (42) respectively.

(ii) If $B_{l0} = 0$ but $B_{h0} \neq 0$, it is $\delta B_h(t) \to 0$ (asymptotically whether initial perturbation $\delta B_h(0) > 0$ or < 0 (Fig. 4 and Fig. 5). This has the consequence that the asymptotic growth rate becomes the same as in the nonmagnetic case.

(iii) If both $B_{h0} \neq 0$and $B_{l0} \neq 0$ with $\delta B_h(t = 0) = \delta B_l(t = 0) > 0$ the magnetic pressure perturbation acts on both sides of the interface but in opposite direction with opposite phase. This has the consequence that the growth rate $\xi_3 = \dot{\xi}_1$ oscillates symmetrically about $\xi_3 = 0$ if $\frac{kV_h^2}{g} = \frac{kV_l^2}{g}$ which increases in amplitude and frequency as the Alfven velocity increases. However, if $\frac{kV_h^2}{g} \neq \frac{kV_l^2}{g}$ the oscillation is asymmetrical about $\xi_3 = 0$.

ACKNOWLEDGEMENTS

This work is supported by the Department of Science & Technology, Govt. of India under grant no. SR/S2/HEP-007/2008. The authors are thankful to the referee for his helpful critical comments which provides improvement in the presentation of the paper.

Appendix:

Let the surface displacement $\eta(x,t)$ in Layzer's model expanded retaining higher powers of x:- $\eta(x,t) = \eta_0(t) + \eta_2(t)x^2 + \eta_4(t)x^4 + \eta_6(t)x^6$.....

The time dependence of the coefficient functions $\eta_i(t)$ one obtained by equating coefficient of $x^i (i = 0, 2, 4, 6...)$ in the expansion of the kinematical condition in powers of x:-

$\frac{\partial\eta(x,t)}{\partial t} - \frac{\partial\phi}{\partial x}\frac{\partial\eta(x,t)}{\partial x} = -\frac{\partial\phi}{\partial y}$

where the velocity potential $\phi(x,y,t) = a_1(t)\cos(kx)e^{-k(y-\eta_0(t))}$

This gives coefficient of x^2:

$\frac{d\eta_2}{dt} = -ka_1\left[3k\eta_2 + \frac{k^2}{2!}\right]$

Coefficient of x^4: $\frac{d\eta_4}{dt} = -ka_1\left[5k\eta_4 - \frac{5}{2}k^2\eta_2^2 - \frac{5}{6}k^3\eta_2 - \frac{k^4}{4!}\right]$

Coefficient of x^6: $\frac{d\eta_6}{dt} = -ka_1\left[7k\eta_6 - 7k^2\eta_2\eta_4 + \frac{7k^4\eta_2^2}{12} + \frac{7k^5\eta_2}{120} - \frac{7k^3\eta_4}{6} + \frac{7k^3\eta_2^3}{6} + \frac{k^6}{6!}\right]$

giving saturation values $(d\eta_i/dt = 0)$:

$k\eta_2 = -k^2/6$;

$k\eta_4 = -k^4/180$;

$k\eta_6 = -k^6/2835$....

References

[1] J. Hecht, U. Alon and D. Shvarts, *Phys. Fluids* **6**, 4019 (1994).

[2] A.L. Velikovich and G. Dimonte, *Phys. Rev. Lett.* **76**, 3112 (1996).

[3] G. Hazak, *Phys. Rev. Lett.* **76**, 4167 (1996).

[4] Qiang Zhang, *Phys. Rev. Lett.* **81**, 3391 (1998).

[5] V.N. Goncharov, *Phy. Rev. Lett.* **88**, 134502 (2002).

[6] Sung-Ik Sohn, *Phy. Rev. E* **67**, 026301 (2003).

[7] D. Layzer, *The Astrophys. J.* **122**, 1 (1955).

[8] M.K.Srivastava,S.V.Lawande,Manoranjan Khan,Chandra Das and B.Chakraborty , *Phys. Fluids B* **4**, 4086 (1992).

[9] R.J.Mason and M.Tabak, *Phys. Rev. Lett.* **80**, 524 (1998).

[10] C.R.Ghezzi,E.M de Gouveia Dal Pino and J.E.Horvath, *The Astrophys. J.* **548**, L193 (2001).

[11] E.M.de Gouveia Dal Pino and W.Benz, *The Astrophys. J.* **410**, 686 (1993).

[12] S. Chandrasekhar, Hydrodynamic and Hydromagnetic Stability, *(Dover Publication Inc.,New York,1981).*

[13] V.Wheatley,D.I.Pullin, and R.Samtaney , *Phys. Rev. Lett.* **95**,125002 (2005).

[14] S.Liberatore and Serge Bouquet *Phys. Fluids* **20**, 116101 (2008).

[15] R.Samtaney, *Phys. Fluids* **15**, L53 (2003).

[16] U.Shumlak and N.F.Roderick, *Phys. Plasmas* **5**, 2384 (1998).

[17] X.M.Qiu,L.Huang and G.D.Jian, *Phys. Plasmas* **10**, 2956 (2003).

[18] Wenlu Zhang,Zhengwei Wu and Ding Li, *Phys. Plasmas* **12**, 042106 (2005).

[19] Zhiyong Qiu,Zhengwei Wu,Jintao Cao and Ding Li, *Phys. Plasmas* **15**, 042305 (2008).

[20] Jintao Cao,Zhengwei Wu,Haijun Ren and Ding Li, *Phys. Plasmas* **15**, 042102 (2008).

[21] Jintao Cao,Zhengwei Wu,Haijun Ren and Ding Li, *Phys. Plasmas* **16**, 062103 (2009).

[22] M.R.Gupta,Sourav Roy,Manoranjan Khan, H.C.Pant,Susmita Sarkar and M.K.Srivastava, *Phys. Plasmas* **16**, 032303 (2009).

[23] Byung -I. Jun,Michael L. Norman and James M. Stone, *The Astrophys. J.* **453**, 332 (1995).

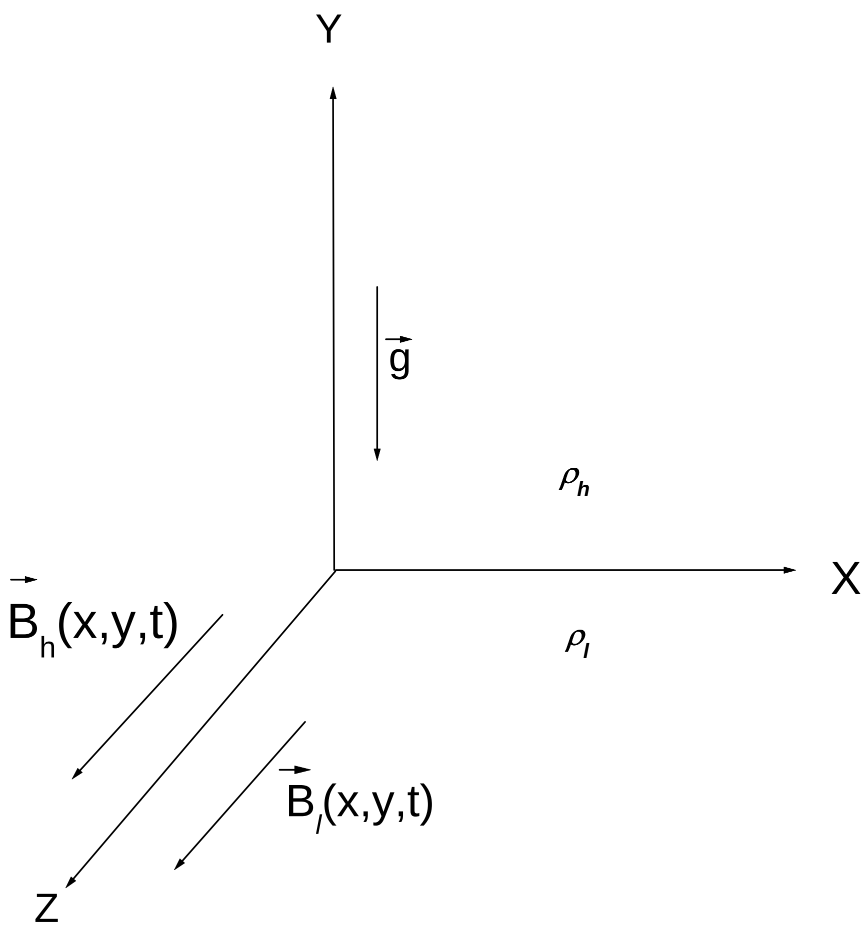

Figure 1: Geometry of the model

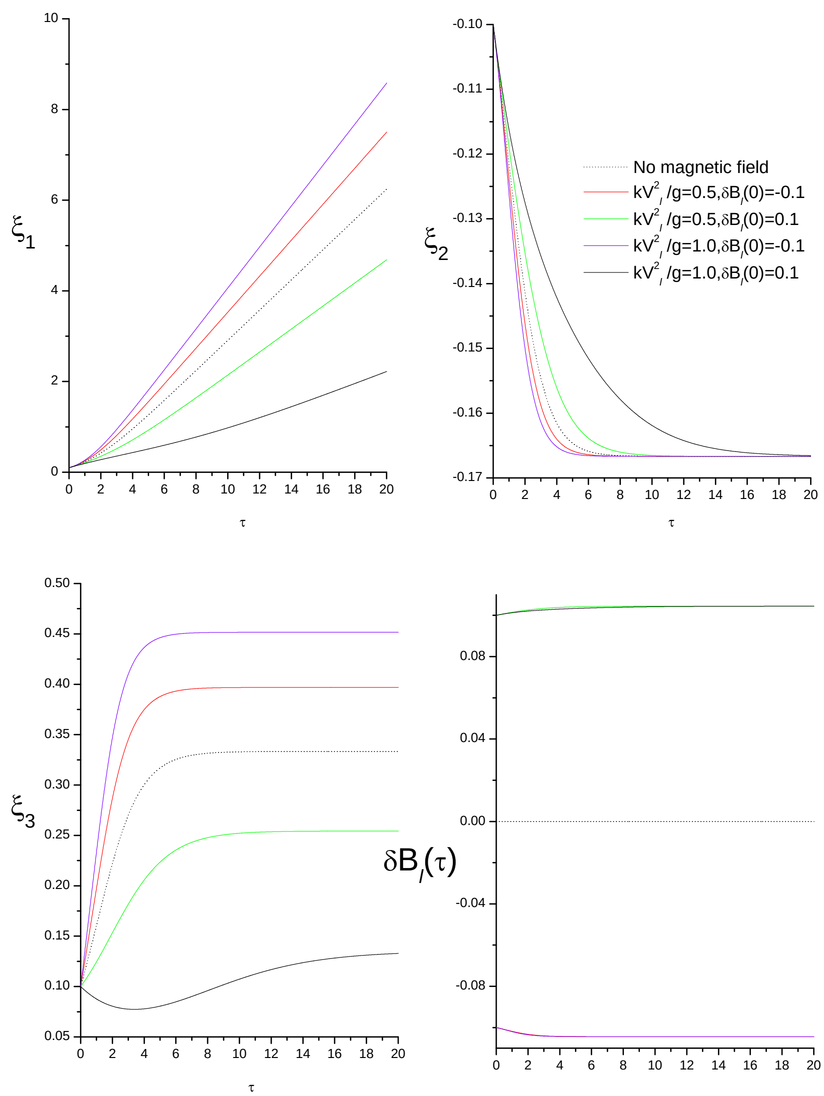

Figure 2: Variation of ξ_1, ξ_2,bubble growth rate $\xi_3(=\dot{\xi}_1)$ and δB_l with τ for $V_h^2 = 0$ [Eq. 36]. Initial values $\xi_1 = 0.1, \xi_2 = -0.1, \xi_3 = 0.1$ and $r = 1.5$

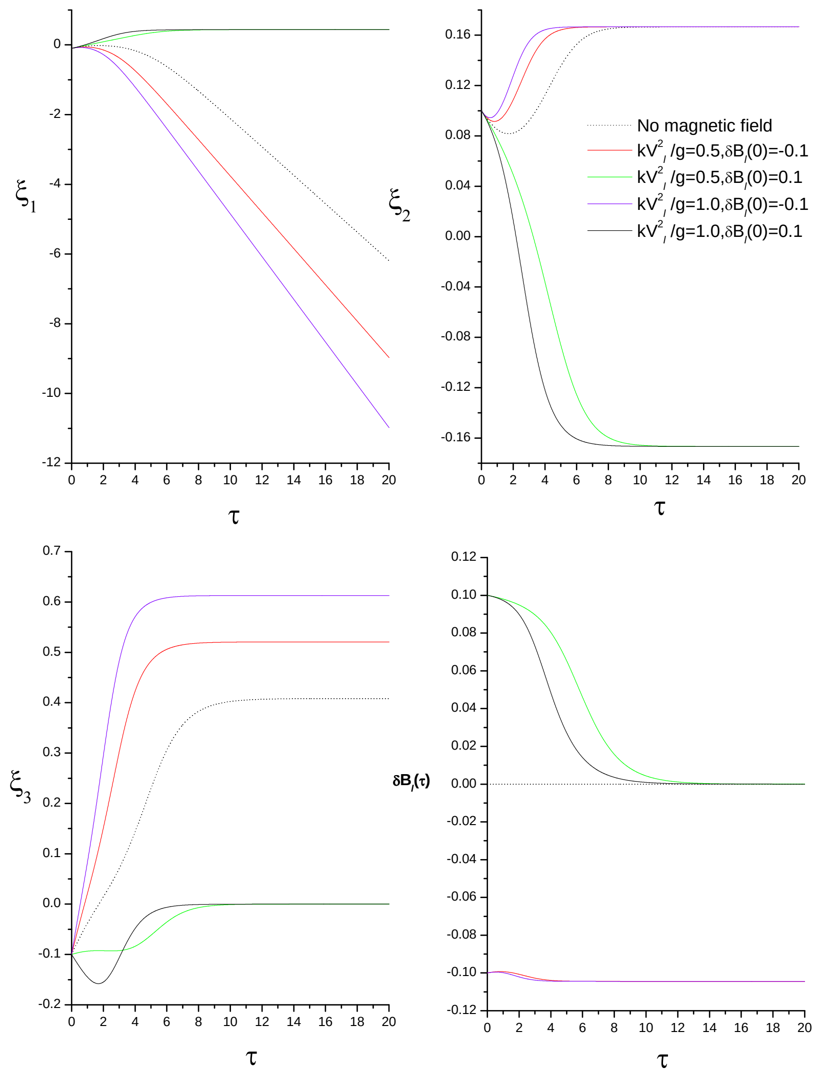

Figure 3: Variation of ξ_1, ξ_2, spike growth rate $\xi_3(=\dot{\xi}_1)$ and δB_l with τ for $V_h^2 = 0$[Eq.36] (with transformation $\xi_1 \rightarrow -\xi_1, \xi_2 \rightarrow -\xi_2, r \rightarrow 1/r$ in Eq.36).Initial values $\xi_1 = -0.1, \xi_2 = 0.1, \xi_3 = -0.1$ and $r = 1.5$

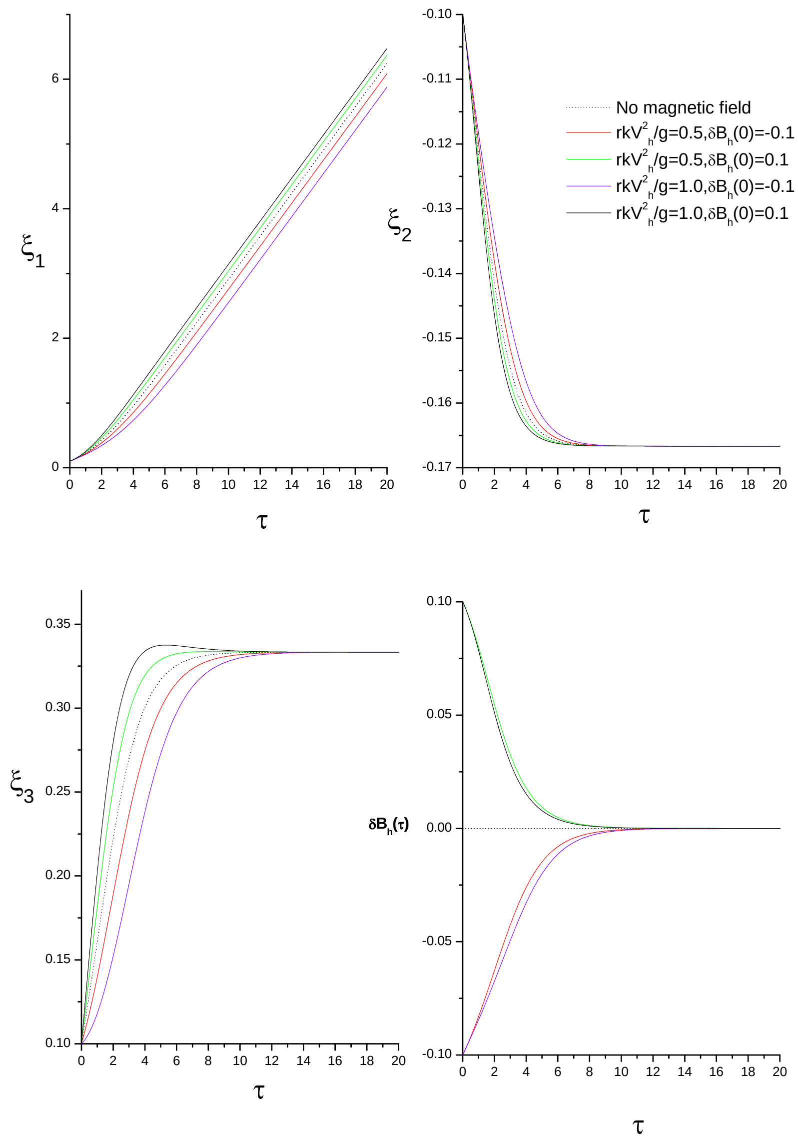

Figure 4: Variation of ξ_1, ξ_2, bubble growth rate $\xi_3(=\dot{\xi}_1)$ and δB_h with τ for $V_l^2 = 0$[Eq.36].Initial values $\xi_1 = 0.1, \xi_2 = -0.1, \xi_3 = 0.1$, and $r = 1.5$

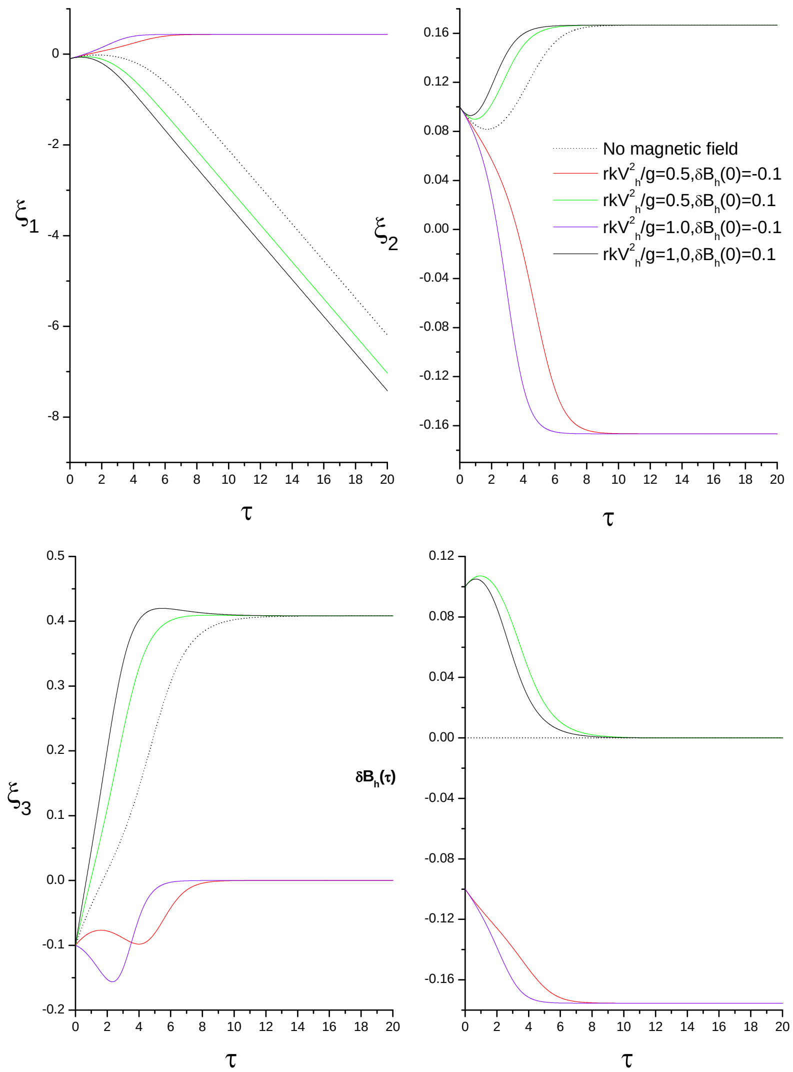

Figure 5: Variation of ξ_1, ξ_2, spike growth rate $\xi_3(=\dot{\xi_1})$ and δB_h with τ for $V_l^2 =$ 0Eq.36 (with transformation $\xi_1 \to -\xi_1, \xi_2 \to -\xi_2, r \to 1/r$ in in Eq.36).Initial values $\xi_1 = -0.1, \xi_2 = 0.1, \xi_3 = -0.1$ and $r = 1.5$

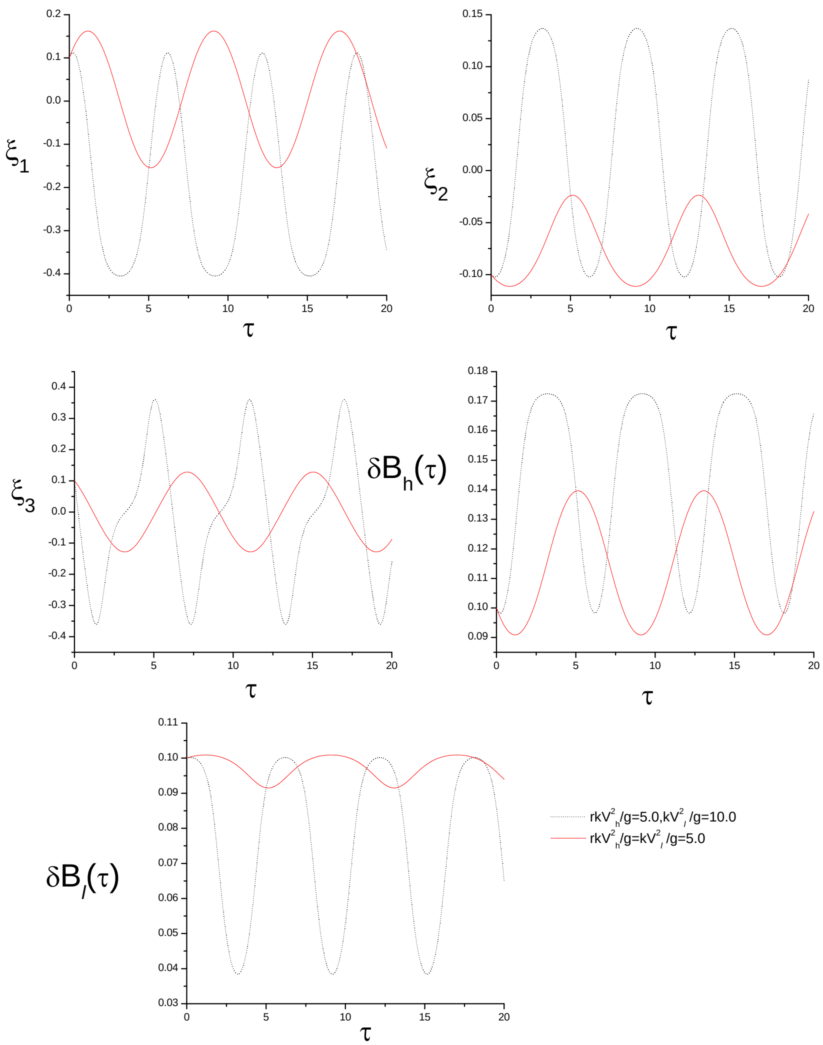

Figure 6: Growth rate oscillations for bubble. Initial values $\xi_1 = 0.1, \xi_2 = -0.1, \xi_3 = 0.1$,$\delta B_l(0) = \delta B_h(0) = 0.1$ and $r = 1.5$

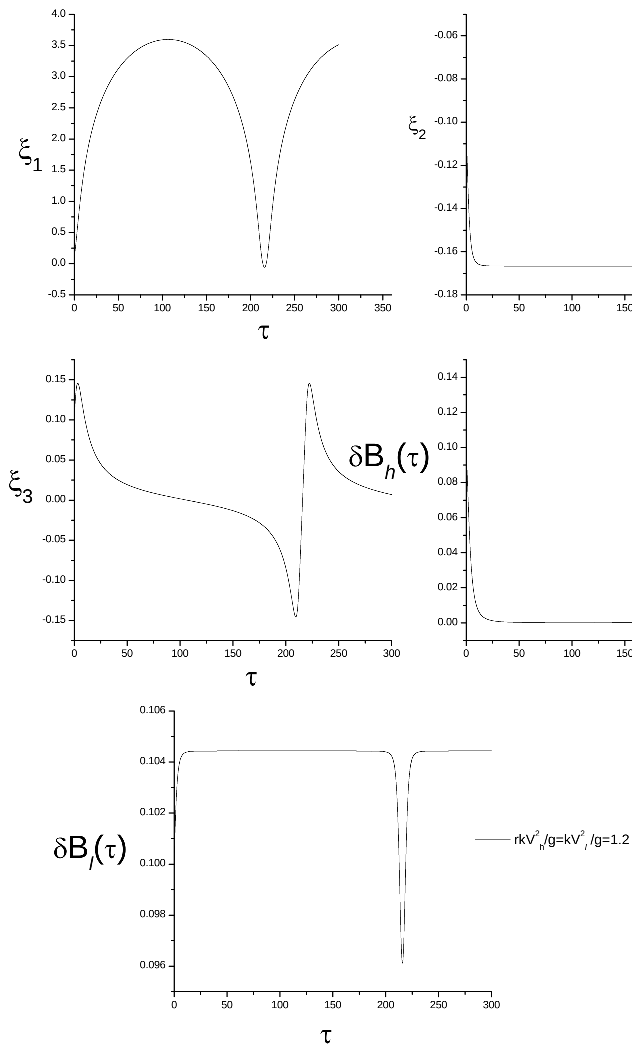

Figure 7: Oscillation of ξ_1, ξ_2, bubble growth rate $\xi_3 (= \dot{\xi}_1)$, δB_h and δB_l with τ as obtained by the solution of Eq. (36) with initial values $\xi_1 = 0.1, \xi_2 = -0.1, \xi_3 = 0.1, \delta B_l(0) = \delta B_h(0) = 0.1$ and $r = 1.5$

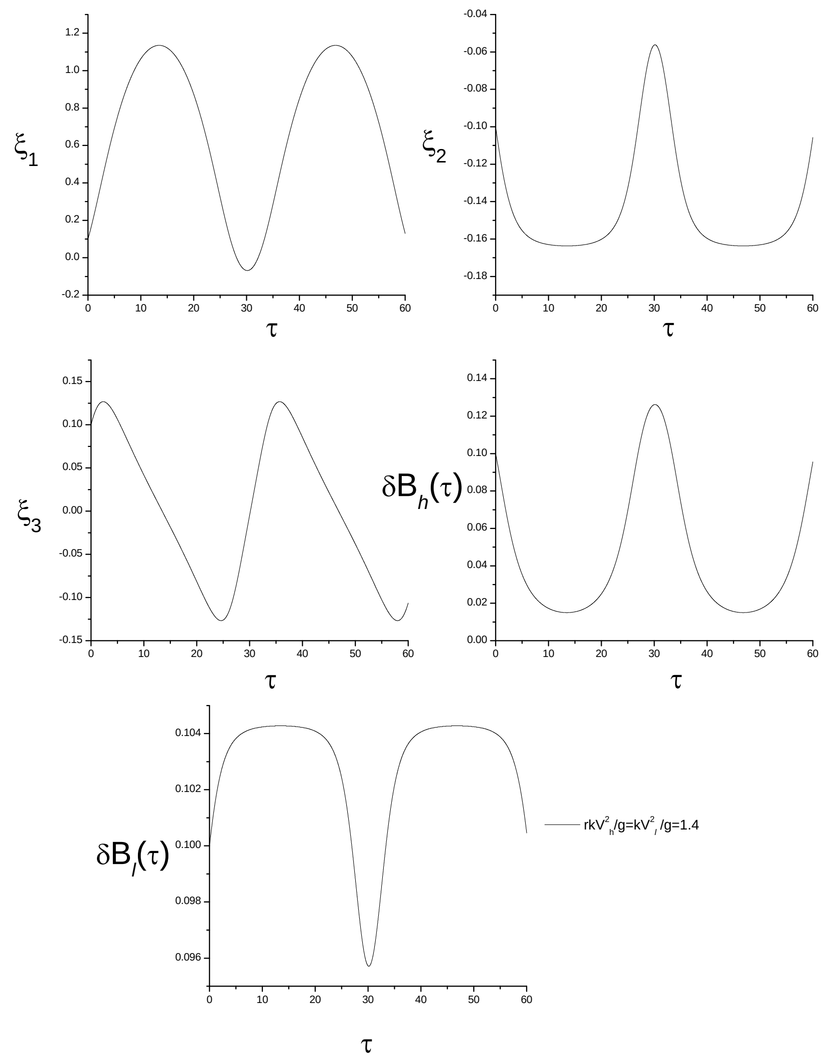

Figure 8: Growth rate oscillation for bubble as obtained by the solution of Eq.(36) with initial values $\xi_1 = 0.1, \xi_2 = -0.1, \xi_3 = 0.1, \delta B_{l1}(0) = \delta B_{h1}(0) = 0.1$ and $r = 1.5$